Accurate Small–Signal Discrete–Time Model of Dual Active Bridge using Saltation Matrices

Rahul Mallik*, Andrew M. Pace*, Samuel A. Burden, and Brian Johnson
Department of Electrical and Computer Engineering, University of Washington, Seattle, WA 98195, USA
Email: {rmallik, apace2, sburden, brianbj}@uw.edu

***Abstract*—The nonlinear nature of dual active bridge (DAB) converters arises from switching between linear dynamics at controlled intervals. In this paper, we model DAB as a hybrid dynamical system consisting of a finite number of modes with linear dynamics and switching surfaces specifying the transition between the modes. In the conventional phase shift modulation (PSM) strategy, the phase shift φ governs the mode transitions and can be used to control DAB output voltage and power. We incorporate φ as a system state and calculate a linearization about a nominal trajectory with so-called saltation matrices that capture the first-order effects of perturbing the states between mode transitions. We demonstrate this linearization provides an accurate discrete-time small-signal model of the DAB.**

***Index Terms*—Hybrid dynamical systems, discrete-time modeling, saltation matrices, dual-active-bridge converters**

I. Introduction

Dual active bridge (DAB) converters are essential in applications where isolation and high voltage conversion ratios are required [1]. The advantages of DAB includes both bidirectional operation and extended zero voltage switching (ZVS) over wide range of power, resulting in low device stress and high power density. While the symmetry of DAB lends itself to very simple control, the large number of switches allows for several intricate pulse width modulation (PWM) control techniques. The performance of these control techniques relies heavily on the underlying model of DAB. The common modeling technique for dc–dc converters is small signal perturbation of the dc state variables around their nominal values [2]. This method however does not apply to DAB due to the presence of high-frequency ac signals in transformer between the two H-bridges.

One of the most common control objectives for DAB is regulating the output dc link voltage. A large signal average model of DAB results in a first order relationship between the phase shift and the output voltage [1], [3]. This model approximates the high-frequency ac variables by the first harmonic [4] and has high fidelity at lower frequencies with the control of the dc voltage being almost perfect. However, such models are not able to accurately predict the state at the different mode transitions within one switching cycle, essential for applications such as ZVS.

A portion of the funding for the work reported in this paper was provided in part by U.S. Department of Energy Office of Energy Efficiency and Renewable Energy Solar Energy Technologies Office grant number DE-EE0008346.

* Rahul Mallik and Andrew M. Pace are co-first authors. Corresponding author is Rahul Mallik.

To obtain higher granularity, sampled-data modeling is a well known alternative to produce a discrete time model of power converters [5] and has been extended to DAB by incorporating auxiliary electromagnetic interference (EMI) filters [6]. The resulting solution of the small signal perturbation is obtained by a linear approximation of the Jacobian with respect to initial condition, changes in terminal voltage and the control variable. Our proposed model, however does not use any linear approximation, and describes the exact matrix solutions to the small signal perturbations of the system. A similar approach based on bilinear approximation of the state transition matrix has been used in [7]. Models like [7] rely on successively appending the state transition matrix with the corresponding dwell times in each of the transition modes. However, as shown in [8], the failure to incorporate the change in dynamics due to switching in the small signal model can lead to errors and controllers based on these faulty models can drive the state trajectories unstable.

In [9], the state transition matrix is combined with superposition of phase shift perturbations to develop a small-signal model for DAB which is in line with the model obtained in this paper. While the method in [9] generates a correct lower order model, it is difficult to generate higher order models or adjust to other PWM control techniques. As the complexity of PWM techniques and model order increases, the method in [9] of adding the resultant perturbations to obtain the complete model becomes extremely tedious. The method proposed in this paper inherently handles this problem by extending the state variable to include the control variable as the $n+1^{\text{th}}$ state, in addition to the usual state variables that describe the dynamics of the DAB.

Our method applies Filippov's method for dc–dc converters to DAB [10]. The underlying method relies on the *saltation matrix* to compute a jump update of the state transition matrix when the operating mode of the dc–dc converter changes. This method has been used to determine stability of other classes of dc–dc converters like interleaved boost converters [11], voltage-mode-controlled buck converter [12], and buck converters [8]. The use of the saltation matrix provides a mathematical structure when calculating the state transition matrix that easily extends to higher order models of DAB. An important contribution of this paper is including the phase shift control parameter φ as a state variable when computing the linearization of the system. Including the control parameter φ in the state of the model, we construct a transfer function

978-1-7281-5826-6/20/$31.00 ©2020 IEEE

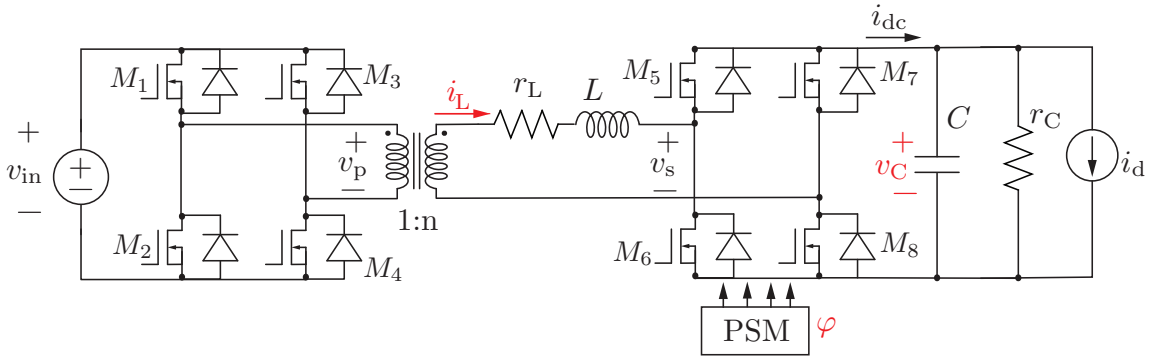

Figure 1. The switched model of DAB is shown with the passive and active components. The phase shift φ is applied to the secondary bridge. The dc load resistance, lumped with the capacitor's parasitic parallel resistance is represented as r_{C}. The current i_{d} represents an active load like an inverter, which can be modelled as a current source.

between the control signal φ and the system state of DAB on a cycle-to-cycle basis.

The paper is organized as follows. In Sec. II a brief background of hybrid dynamic systems as applicable to DAB is presented. Sec. III provides the main result of the paper, a derivation of the cycle–by–cycle small–signal model of DAB; followed by a verification of the model in Sec. IV using PLECS.

II. Background on Hybrid Dynamical Systems Theory

Hybrid dynamical systems describe systems where the underlying continuous dynamics change at discrete instances. *Switched linear systems* are a subset of hybrid dynamical systems where the dynamics for each discrete mode is linear. The dynamics of DAB, with discrete changes in the underlying linear dynamics of the continuous state, can be modeled as a switched linear system. A brief overview of the dynamics and relevant results for switched systems follows, a more thorough overview is provided in [13], [14].

Let $x \in \mathbb{R}^n$ denote the state of the system with dynamics $\dot{x}(t) = f_k(t, x(t))$, where $f_k \colon \mathbb{R}^n \to \mathbb{R}^n$ is globally Lipschitz continuous and $k \in \{1, \ldots, N\}$ denote the discrete mode of the system with $N \in \mathbb{N}$. The *switching surface* between two modes k and j is given by $\mathcal{G}(t) = \{x \mid g_{k,j}(t, x) = 0\} \subset \mathbb{R}^n$, where $g_{k,j} \colon \mathbb{R}^+ \times \mathbb{R}^n \to \mathbb{R}$ and at least once differentiable. When $x(t) \in \mathcal{G}_{k,j}(t)$ the discrete mode of the system changes from j to k.

In a continuous linear system, the result of a perturbation on the initial condition of a nominal trajectory $x(t)$ is calculated with the state transition matrix Φ. In order to calculate a linearization for a switched system, the discrete changes in the underlying dynamics must be accounted for. The *saltation* matrix, originally described in [15], calculates the first order effects of switching the discrete mode and hence changing the continuous dynamics at a different time than the nominal trajectory due to a perturbation in the continuous state. The saltation matrix $\mathbf{S}_{k,j}$ for switching between discrete modes j and k is [16, Sec. 3]

$$\mathbf{S}_{k,j}(t,x) = I + \frac{\Big(f_k(t,x) - f_j(t,x)\Big) Dg_{k,j}(t,x)}{Dg_{k,j}(t,x) f_j(t,x) + \frac{\partial g_{k,j}}{\partial t}(t,x)}, \tag{1}$$

where t, x are the time and state when the switching surface is reached, $g_{k,j}(t,x) = 0$ and $Dg_{k,j}$ is the derivative of the switching function $g_{j,i}$ with respect to the state x. A key criteria for the use of saltation matrix is the trajectory $x(t)$ is transverse to the switching surface in the (t,x) plane at the point of intersection, $Dg_{k,j}(t,x) f_j(t,x) + \frac{\partial g_{k,j}}{\partial t} \neq 0$.

With this terse background on saltation matrices, we now proceed to model DAB as a switched linear system.

III. Discrete Time Modeling of Dual Active Bridge

DAB uses simple phase-shift modulation since it (theoretically) guarantees ZVS when the ratio of the output voltage to the input voltage is exactly equal to the transformer turns ratio. The DAB circuit in Fig. 1 utilizes PSM where the secondary-side phase shift φ is defined relative to the primary-side switch signal. For a given phase shift φ between high frequency ac voltages of the two bridges, the exact power balance equation is given by

$$\underbrace{\frac{n^2 v_{\mathrm{in}}^2 \varphi\,(\pi - \varphi)}{L \pi \omega_{\mathrm{sw}}}}_{\text{Input power}} = \underbrace{\left(\frac{n v_{\mathrm{in}} \varphi}{L \omega_{\mathrm{sw}}}\right)^2 \left(1 - \frac{2\varphi}{3\pi}\right) r_{\mathrm{L}}}_{\text{Loss in inductor ESR}} + \underbrace{\frac{n^2 v_{\mathrm{in}}^2}{r_C} + n v_{\mathrm{in}} i_{\mathrm{d}}}_{\text{Power Output}}, \tag{2}$$

where n is the transformer turns ratio, L is the inductance and r_{L} the equivalent series resistance of the secondary-side magnetics which can be extended without loss of generalization to also include the device on state resistances. The net resistive load at the output (the parallel combination of the capacitance parasitic resistance and load resistor) is denoted by r_{C}, ω_{sw} is the switching frequency and i_{d} is the equivalent current source model for an active load like an inverter.

We use (2) to solve for a particular phase shift φ that ensures dc transformer mode of operation of the DAB, thereby regulating the output voltage v_{C} to be equal to nv_{in}. This defines a nominal state trajectory in every switching cycle with discrete mode transitions in it as shown in Fig. 2 (b).

Next, we construct a linearization about the nominal equilibrium trajectory. The linearization describes to first order how perturbation of the state and control parameter at the start of a cycle map to the perturbed values at the start of the next cycle. Letting x denote the nominal state of the system at the start of a cycle, and φ denote the control parameter that achieves this nominal state, we seek to find the mapping

$$\Delta x[\ell+1] = F\Delta x[\ell] + G\Delta\varphi[\ell], \tag{3}$$

with

$$\Delta x[\ell] = x[\ell] - x, \quad \Delta\varphi[\ell] = \varphi[\ell] - \varphi, \tag{4}$$

and $x[\ell], \varphi[\ell]$ being the state and control parameter respectively at the start of the cycle. In dynamical system terminology, we aim to construct the first order approximation of the Poincaré map [17, Chp. 10].

A. Switched Linear System Formulation

As a first step towards linearization, we define the dynamics as a switched linear system. The two main components are (1) defining the set of linear dynamics and (2) defining the discrete transitions between the linear dynamics. We begin by defining the state vector as $x = \begin{bmatrix} i_{\mathrm{L}} & v_{\mathrm{C}} \end{bmatrix}^T$ with i_{L} the inductor current and v_{C} the output voltage and indicated in Fig. 1. The state x evolves with the dynamics

$$\begin{aligned} \frac{di_{\mathrm{L}}}{dt} &= \frac{s_1 n v_{\mathrm{in}}}{L} - \frac{s_2 v_{\mathrm{C}}}{L} - \frac{r_{\mathrm{L}} i_{\mathrm{L}}}{L}, \\ \frac{dv_{\mathrm{C}}}{dt} &= \frac{s_2 i_{\mathrm{L}}}{C} - \frac{v_{\mathrm{C}}}{r_{\mathrm{C}} C} - \frac{i_{\mathrm{d}}}{C}, \end{aligned} \tag{5}$$

where the switching signals s_1, s_2, shown in Fig. 2(a), are defined as

$$s_1(t) = \begin{cases} 1, & 0 \le \omega t < \pi \\ -1, & \pi \le \omega t < 2\pi \end{cases}, \tag{6}$$

$$s_2(t) = \begin{cases} 1, & \varphi \le \omega t < \pi + \varphi \\ -1, & 0 \le t < \varphi \text{ and } \pi + \varphi \le \omega t < 2\pi. \end{cases} \tag{7}$$

It follows there are four discrete modes consisting of linear dynamics in the system.

Assuming v_{in} and i_{d} remain constant over a cycle, the dynamics in each mode can succinctly be written as

$$\dot{x}(t) = A_k x + B_k u_\ell,$$

where $A_k \in \mathbb{R}^{2\times 2}$ and $B_k \in \mathbb{R}^2$ are the matrix representation of the state dynamics in (5) and $u_\ell = \begin{bmatrix} v_{\mathrm{in}} & i_{\mathrm{d}} \end{bmatrix}^T$. Explicitly writing out the equation gives

$$\underbrace{\frac{d}{dt}\begin{bmatrix} i_{\mathrm{L}} \\ v_{\mathrm{C}} \end{bmatrix}}_{\dot{x}} = \underbrace{\begin{bmatrix} -\frac{r_{\mathrm{L}}}{L} & -\frac{s_2}{L} \\ \frac{s_2}{C} & -\frac{1}{r_{\mathrm{C}} C} \end{bmatrix}}_{A_k} \underbrace{\begin{bmatrix} i_{\mathrm{L}} \\ v_{\mathrm{C}} \end{bmatrix}}_{x} + \underbrace{\begin{bmatrix} \frac{s_1 n}{L} & 0 \\ 0 & -\frac{1}{C} \end{bmatrix}}_{B_k} \underbrace{\begin{bmatrix} v_{\mathrm{in}} \\ i_{\mathrm{d}} \end{bmatrix}}_{u_\ell}. \tag{8}$$

DAB operation begins in mode $k = 1$ with the switching signal $(s_1, s_2) = (1, -1)$. This switching signal indicates the MOSFETs M_1, M_4 are turned on in the input bridge causing v_{p} to be equal to the input voltage. Meanwhile in the output bridge, the MOSFETs M_6, M_7 are turned on, causing the secondary bridge voltage v_{s} to be equal to $-v_{\mathrm{C}}$. The other mode dynamics can be similarly explained. The output voltage v_{C} is controlled at nv_{in} causing the inductor current i_{L} to be trapezoidal.

The scalar control variable φ for DAB changes the relative switching phase between modes $k = 1$ to $k = 2$ and modes $k = 3$ to $k = 4$.[1] To construct a linearization with the scalar control variable included, we augment the existing state vector with a parameter for the phase shift φ. As the phase shift does not change during the cycle, the dynamics of the control parameter are described with $\dot{\varphi} = 0$. The resulting state of the system is then $\tilde{x} = \begin{bmatrix} i_L & v_c & \varphi \end{bmatrix}^T$. The switching surfaces between each of the modes are

$$g_{2,1}(t, \tilde{x}) = 2\pi t / T_{\mathrm{sw}} - \varphi, \tag{9}$$

$$g_{3,2}(t, \tilde{x}) = 2\pi t / T_{\mathrm{sw}} - \pi, \tag{10}$$

$$g_{4,3}(t, \tilde{x}) = 2\pi t / T_{\mathrm{sw}} - (\pi + \varphi), \tag{11}$$

$$g_{1,4}(t, \tilde{x}) = 2\pi t / T_{\mathrm{sw}} - 2\pi. \tag{12}$$

For each mode $k \in \{1, 2, 3, 4\}$, t_k denotes the switching time such that the switching function, $g_{k+1,k}(t_k, \tilde{x}) = 0$ and a change from mode k to mode $k+1$.As each of the continuous mode dynamics is linear, the state transition matrix $\Phi_k \in \mathbb{R}^{3\times 3}$ is given by[2]

$$\Phi_k = \exp\left(\begin{bmatrix} A_k & 0_{2\times 1} \\ 0_{1\times 2} & 0 \end{bmatrix}(t_{k+1} - t_k)\right) \tag{13}$$

captures the necessary linearization, where $\exp(\cdot)$ denotes the matrix exponential.

B. Computing the First Order Model

The saltation matrix for a transition between the present discrete mode, k, and its immediate next discrete mode, $k+1$, is reproduced from (1) as,

$$\mathbf{S}_{k+1,k}(t, \tilde{x}) = I + \frac{\Big(f_{k+1}(t, \tilde{x}) - f_k(t, \tilde{x})\Big) Dg_{k+1,k}(t, \tilde{x})}{Dg_{k+1,k}(t, \tilde{x}) f_k(t, \tilde{x}) + \frac{\partial g_{k+1,k}}{\partial t}(t, \tilde{x})}. \tag{14}$$

The state dynamics $f_k(t, \tilde{x})$ for a particular discrete mode k is written as,

$$f_k(t, \tilde{x}) = \begin{bmatrix} A_k & 0_{2\times 1} \\ 0_{1\times 2} & 0 \end{bmatrix}\tilde{x} + \begin{bmatrix} B_k \\ 0_{1\times 2} \end{bmatrix} u_\ell. \tag{15}$$

$Dg_{k+1,k}(t, \tilde{x})$ is the derivative of the switching function $g_{k+1,k}(t, \tilde{x})$ at the point on the switching surface $(t, \tilde{x})$. As an example, evaluated for the first transition between mode $k = 1$ and $k = 2$, $Dg_{2,1}(t, \tilde{x}) = \begin{bmatrix} 0 & 0 & -1 \end{bmatrix}^T$. It can be

[1] The switching phase between mode $k = 2$ to $k = 3$ is fixed at π; likewise fixed at 2π for switching between mode $k = 4$ to $k = 1$.

[2] A matrix with all 0 elements of size $m \times n$ is denoted with $0_{m\times n}$ and the identity matrix of size $n \times n$ denoted with $I_{n\times n}$.

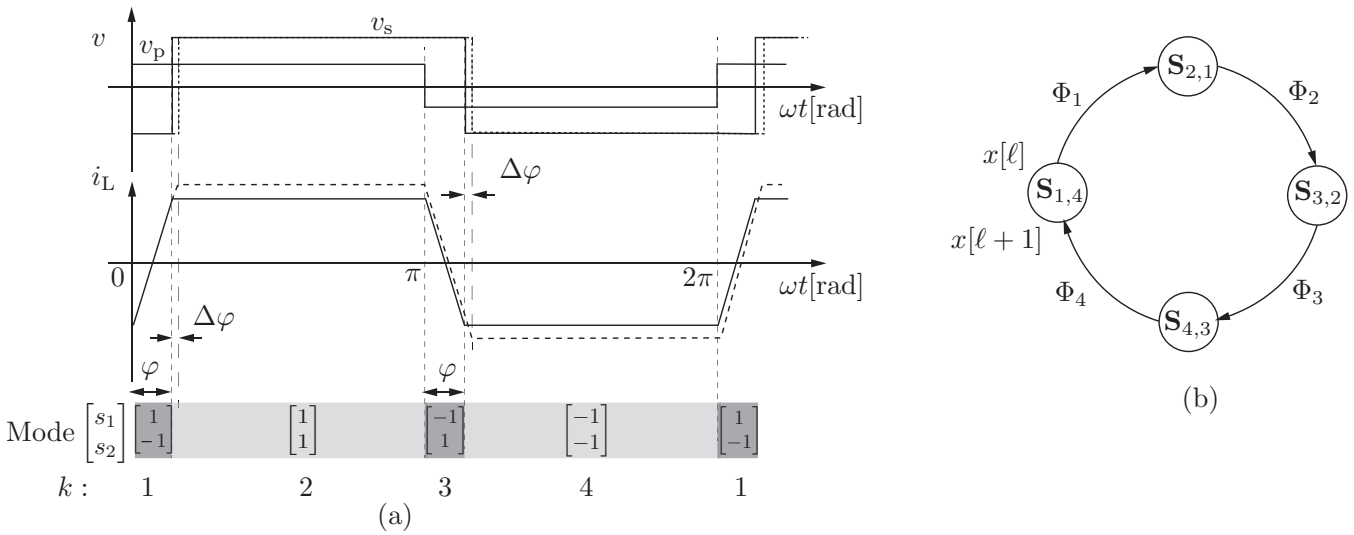

Figure 2. For each of the mode transitions k we draw the primary and secondary side transformer voltages and inductor current in (a). The nominal phase shift is φ and the perturbation in the phase shift $\Delta\varphi$ is used to obtain the perturbed state trajectory as shown in dotted lines. For any state variable $x[\ell]$, the value of the state variable at the end of one switching cycle can be obtained by the product of matrix exponentials and saltation matrices as shown in (b).

evaluated similarly for the other mode transitions.

In the next step, we evaluate the time derivative of the switching surface $g_{k+1,k}(t,\tilde{x})$. This derivative for the first mode transition is

$$\frac{\partial g_{2,1}(t,x)}{\partial t} = \frac{2\pi}{T_{\text{sw}}}, \tag{16}$$

and is equal for all other mode transitions. Once all the variables have been obtained, we substitute them in (14) and obtain the saltation matrix in terms of the system matrices as

$$\mathbf{S}_{k+1,k}\left(t_k,\tilde{x}\right) = \begin{bmatrix} I_{2\times 2} & \frac{(A_{k+1}-A_k)x+(B_{k+1}-B_k)u_\ell}{-2\pi/T_{\text{sw}}} \\ 0_{1\times 2} & 1 \end{bmatrix}, \tag{17}$$

for $k \in \{1,3\}$. As neither $g_{3,2}$ nor $g_{1,4}$ depend on the state $\tilde{x}$, $Dg_{3,2}(t,\tilde{x}) = Dg_{1,4}(t,\tilde{x}) = 0$ giving $\mathbf{S}_{3,2} = \mathbf{S}_{1,4} = I$. Incorporating the saltation matrix as in Fig. 2(b), the linearization for one period is

$$\begin{aligned} \Phi &= \mathbf{S}_{1,4}\Phi_4\mathbf{S}_{4,3}\Phi_3\mathbf{S}_{3,2}\Phi_2\mathbf{S}_{2,1}\Phi_1 \\ &= \Phi_4\mathbf{S}_{4,3}\Phi_3\Phi_2\mathbf{S}_{2,1}\Phi_1, \end{aligned} \tag{18}$$

where $\Phi \in \mathbb{R}^{3\times 3}$. The resulting matrix is sometimes referred to as the *monodromy* matrix. Carrying out the calculation yields

$$\Phi = \begin{bmatrix} F & G \\ 0_{1\times 2} & 1 \end{bmatrix}, \tag{19}$$

with $F \in \mathbb{R}^{2\times 2}$ and $G \in \mathbb{R}^{2\times 1}$. As $\Phi\Delta\tilde{x}[\ell] = \Delta\tilde{x}[\ell+1]$, we obtain the desired linearization

$$\Delta x[\ell+1] = F\Delta x[\ell] + G\Delta\varphi[\ell], \tag{20}$$

where Δx and $\Delta\varphi$ are as described in (4).

C. Computing the Transfer Functions

The small signal model obtained in (20) is useful for state space based controller design like linear quadratic regulator or controller based on norm minimization techniques like H_2 and H_∞ control. For classical control techniques like loop shaping design, constructing bode plots from (20) is more useful.

As an important application, dc-link voltage control of DAB requires the transfer function between the perturbation in output voltage Δv_{C} and the perturbation in phase shift $\Delta\varphi$. We obtain $H_{\Delta v_{\text{C}},\Delta\varphi}$ by taking the Z-transform of (20),

$$H_{\Delta v_{\text{C}},\Delta\varphi} = C(zI - F)^{-1}G, \tag{21}$$

where $C = \begin{bmatrix} 0 & 1 \end{bmatrix}$. To verify the proposed modeling strategy, we also derive the transfer function between the perturbation in inductor current, Δi_{L}, sampled at the beginning of transition from mode $k = 4$ to mode $k = 1$ and the perturbation in phase shift, $\Delta\varphi$. This transfer function, $H_{\Delta i_{\text{L}},\Delta\varphi}$ is similar to (21) with C changed to $C = \begin{bmatrix} 1 & 0 \end{bmatrix}$. We verify the transfer functions using the Impulse Response Analysis tool of PLECS. Once the transfer functions are obtained, the controller design is straight-forward and extensively covered in literature [4], [6], [9].

IV. Results and Discussion

To validate the small signal model obtained by the saltation matrix, we setup a PLECS simulation reflecting the theoretical model shown in Fig. 1 with parameters given in Table I. The obtained discrete small signal model from (20) is

$$F = \begin{bmatrix} 0.9260 & 0.0055 \\ 0.0007 & 0.9990 \end{bmatrix}, \quad G = \begin{bmatrix} -0.8560 \\ 0.4851 \end{bmatrix}. \tag{22}$$

To validate elements of the G matrix, we perturb the input and observe the perturbation in the corresponding output. Fig. 4

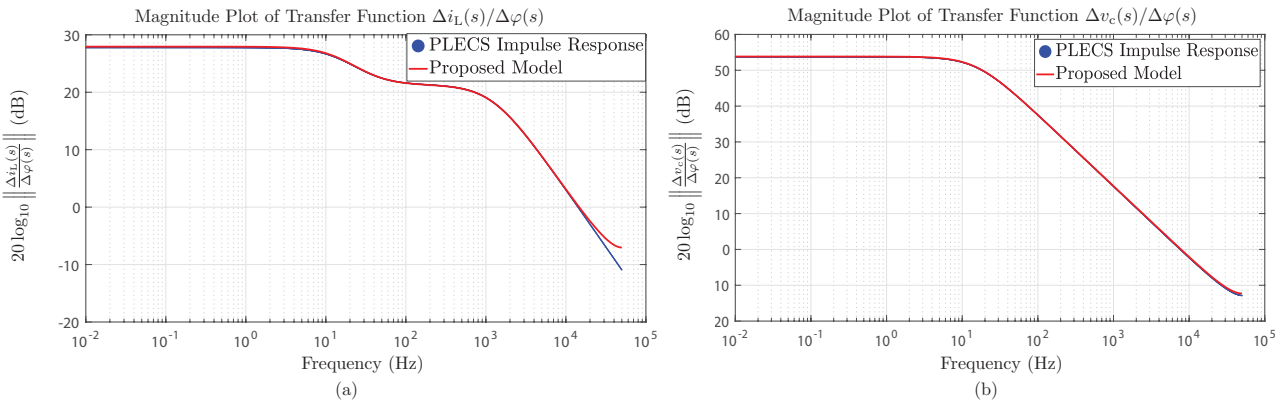

Figure 3. Bode plots of the transfer function calculated using the modelling approach in Sec. III closely match the corresponding bode plot generated using PLECS. The two bode plots presented are of the transfer function $\Delta i_{\mathrm{L}}(s)/\Delta\varphi(s)$ in (a) and $\Delta v_{\mathrm{C}}(s)/\Delta\varphi(s)$ in (b).

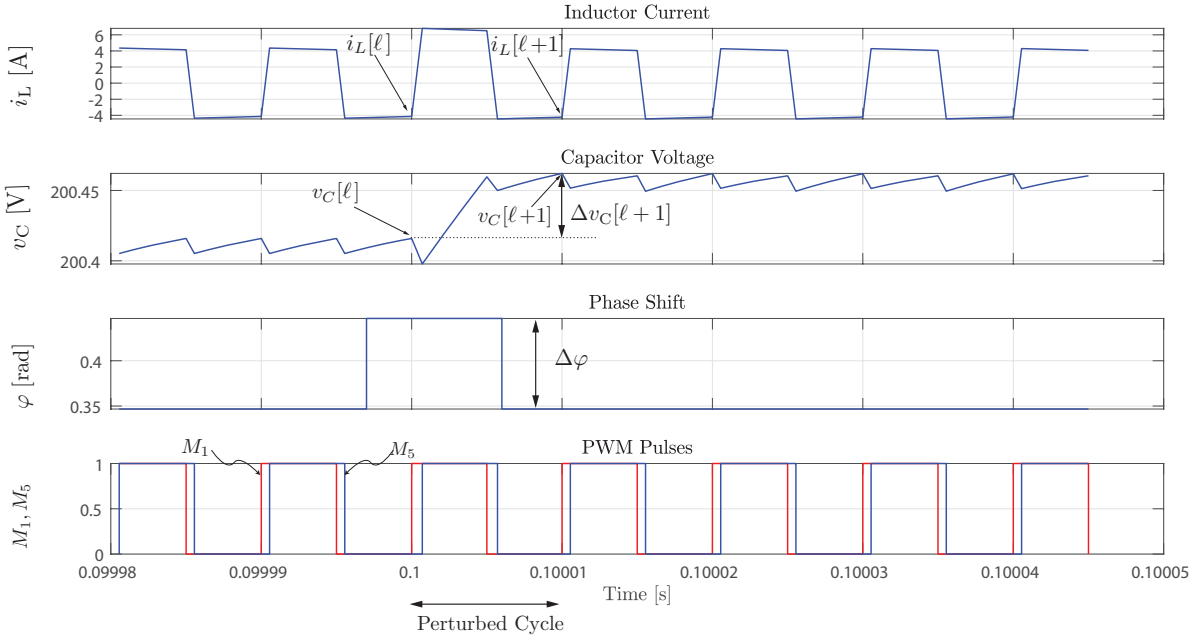

Figure 4. The numerically calculated G (22) is validated by perturbing the switching phase φ by a nonzero amount in a PLCES simulation. A nonzero perturbation of the switching phase φ occurs in the cycle starting at time 0.1 s and the change in the two states, the inductor current i_{L} and the capacitor voltage v_{C}, at the start of this cycle and the start of the subsequent cycle starting at $t = 0.10001$ s is measured. While not necessary for the validation, the plots show the inductor current i_{L} rapidly returning to steady state after the phase perturbation is removed and the slower response of the capacitor voltage v_{C}. The PWM pulses show the gate signals of switches M_1 and M_5 as shown in Fig. 1.

demonstrates this validation process where the phase φ is perturbed. First the system reaches steady state by time 0.1 s with a nominal phase shift φ calculated by the power balance equation (2). Then, we apply a small perturbation to the phase shift $\Delta\varphi$ over a single cycle starting at 0.1 s. We measure the effect of the perturbation on the two state variables, inductor current i_{L} and capacitor voltage v_{C}, at the start of the next cycle 0.10001 s by computing $\Delta i_{\mathrm{L}}[\ell+1]$ and $\Delta v_{\mathrm{C}}[\ell+1]$, and then calculate

$$G = \begin{bmatrix} \Delta i_{\mathrm{L}}[\ell+1]/\Delta\varphi \\ \Delta v_{\mathrm{C}}[\ell+1]/\Delta\varphi \end{bmatrix}. \tag{23}$$

The results from (23) is then compared with (22). A similar procedure can be carried out to validate the elements of the F matrix by perturbing the initial states.

Another way of verifying the model is to obtain the bode plot of the transfer function as described by (21) and compare it with the bode plot generated by the impulse response tool of the PLECS. With the existing simulation which mimics our theoretical model and parameters from Table I. Fig. 3(a) shows the close match of the bode plot of the transfer function between the perturbation in inductor current at the beginning of mode $k = 1$ to the perturbation in phase shift, as predicted

Table I
DAB SYSTEM PARAMETERS

Symbol	Description	Value	Units
v_{in}	Input Voltage	200	V
L	Filter inductance	26	μH
r_{L}	Inductor ESR	0.2	Ω
C	Filter capacitance	200	μF
n	Transformer turns ratio	1	–
r_{C}	Load resistance	53.2	Ω
i_{d}	Load current	0	A

by the proposed model (in red) to the impulse response of the PLECS model (in blue). The transfer function of the perturbation in capacitor voltage to the perturbation in phase shift shown in Fig. 3(b) also shows a good match between the two bode plots.

A. Symbolic Representation of the Linear Model

The main advantage of the proposed controller is to obtain a small signal model of the perturbations of the state variable with the perturbation of the control variable. So in a controller synthesized based on LQR or pole placement, the reference to the controller would only be the change in state variables that we would like to observe. However, as the system adjusts to the new reference, the new nominal trajectory now needs to have the F and G matrices recomputed. In an online power converter, it might not be computationally efficient to implement (18).

One approach is to do a sensitivity analysis on the nominal plant and try to observe how much do the elements of the F and G matrix vary from its nominal computed values. Another approach is to approximate (18) by substituting the first order approximation for the matrix exponential $\exp(At) \approx I + At$ giving

$$\hat{F} = \begin{bmatrix} 1 - \frac{r_{\text{L}} T_{\text{sw}}}{L} & (\varphi - \frac{1}{4})\Big(\frac{L - C r_{\text{C}} r_{\text{L}}}{C L^2 r_{\text{C}}}\Big) T_{\text{sw}}^2 \\ (\varphi - \frac{1}{4})\Big(\frac{L - C r_{\text{C}} r_{\text{L}}}{C^2 L r_{\text{C}}}\Big) T_{\text{sw}}^2 & 1 - \frac{T_{\text{sw}}}{r_{\text{C}} C} \end{bmatrix} + \mathcal{O}(T_{sw}^3) \tag{24}$$

$$\hat{G} = \begin{bmatrix} -\frac{n r_{\text{L}} T_{\text{sw}}^2 v_{\text{in}}}{2\pi L^2} \\ \frac{n T_{\text{sw}}^2 v_{\text{in}} (\pi - \varphi)}{\pi^2 L C} \end{bmatrix} + \mathcal{O}(T_{sw}^3). \tag{25}$$

Since we use a very high switching frequency to control the DAB, T_{sw} is numerically very small and the errors accumulated due to ignoring of higher order terms is also small. The bode plots obtained from the actual model (20) and the one approximated by $\hat{F}$ and $\hat{G}$ line up very closely throughout the frequency range from low frequency, 10^{-3} Hz, to the Nyquist frequency, $0.5 T_{\text{sw}}$.

V. CONCLUSION AND FUTURE WORK

In this paper, we have obtained an accurate discrete time model of DAB taking into account the switching dynamics using saltation matrices. We validated the proposed modeling approach by comparing the predictions from the model with a commercial simulation software for both impulse response and perturbation analysis. We also presented a symbolic expression the approximates the model which can be used in real time. As possible future work, the developed model can be used to to construct state–space controllers like linear quadratic regulator and minimal norm based controllers for DAB. An extension in terms of modeling is also possible by incorporating more state variables in this modeling framework.

REFERENCES

[1] R. W. De Doncker, D. M. Divan, and M. H. Kheraluwala, "A three-phase soft-switched high power density dc/dc converter for high power applications," in *IEEE Industry Applications Society Annual Meeting*, Oct 1988.

[2] R. Erickson and D. Maksimovic, *Fundamentals of Power Electronics*. Springer, 2001.

[3] R. Mallik, B. Majmunovic, S. Mukherjee, S. Dutta, G. . Seo, D. Maksimovic, and B. Johnson, "Equivalent circuit models of voltage-controlled dual active bridge converters," in *2019 20th Workshop on Control and Modeling for Power Electronics (COMPEL)*, pp. 1–4, 2019.

[4] J. A. Mueller and J. W. Kimball, "An improved generalized average model of dc–dc dual active bridge converters," *IEEE Transactions on Power Electronics*, vol. 33, Nov 2018.

[5] G. C. Verghese, M. E. Elbuluk, and J. G. Kassakian, "A general approach to sampled-data modeling for power electronic circuits," *IEEE Transactions on Power Electronics*, April 1986.

[6] F. Krismer and J. W. Kolar, "Accurate small-signal model for the digital control of an automotive bidirectional dual active bridge," *IEEE Transactions on Power Electronics*, Dec 2009.

[7] L. Shi, W. Lei, Z. Li, J. Huang, Y. Cui, and Y. Wang, "Bilinear discrete-time modeling and stability analysis of the digitally controlled dual active bridge converter," *IEEE Transactions on Power Electronics*, vol. 32, pp. 8787–8799, Nov 2017.

[8] D. Giaouris, S. Banerjee, B. Zahawi, and V. Pickert, "Stability Analysis of the Continuous-Conduction-Mode Buck Converter Via Filippov's Method," *IEEE Transactions on Circuits and Systems I: Regular Papers*, vol. 55, pp. 1084–1096, May 2008.

[9] D. Costinett, R. Zane, and D. Maksimović, "Discrete-time small-signal modeling of a 1 mhz efficiency-optimized dual active bridge converter with varying load," in *IEEE Workshop on Control and Modeling for Power Electronics (COMPEL)*, pp. 1–7, June 2012.

[10] K. Mandal, S. Banerjee, and C. Chakraborty, "A New Algorithm for Small-Signal Analysis of DC–DC Converters," *IEEE Transactions on Industrial Informatics*, pp. 628–636, Feb. 2014.

[11] H. Wu, V. Pickert, and D. Giaouris, "Nonlinear analysis for interleaved boost converters based on Monodromy matrix," in *IEEE Energy Conversion Congress and Exposition (ECCE)*, pp. 2511–2516, Sept. 2014.

[12] D. Giaouris, S. Maity, S. Banerjee, V. Pickert, and B. Zahawi, "Application of Filippov method for the analysis of subharmonic instability in dc-dc converters," *International Journal of Circuit Theory and Applications*, vol. 37, pp. 899–919, Oct. 2009.

[13] M. S. Branicky, "Introduction to Hybrid Systems," in *Handbook of Networked and Embedded Control Systems*, pp. 91–116, Boston, MA: Birkhäuser, 2005.

[14] A. J. van der Schaft and J. M. Schumacher, *An Introduction to Hybrid Dynamical Systems*. Springer, 2000.

[15] M. A. Aizerman and F. R. Gantmacher, "Determination of Stability by Linear Approximation of a Periodic Solution of a System of Differential Equations with Discontinuous Right-Hand Sides," *The Quarterly Journal of Mechanics and Applied Mathematics*, vol. 11, no. 4, 1958.

[16] R. I. Leine, D. H. Van Campen, and B. L. Van De Vrande, "Bifurcations in Nonlinear Discontinuous Systems," *Nonlinear Dynamics*, vol. 23, 2000.

[17] M. W. Hirsch, S. Smale, and R. L. Devaney, *Differential Equations, Dynamical Systems, and an Introduction to Chaos*. Elsevier, 2013.